JOURNAL OF SCIENCE AND TECHNOLOGY VOL. 12 NO. 1 (2020) 15-28

JST

Journal homepage: http://penerbit.uthm.edu.my/ojs/index.php/jst
ISSN : 2229-8460 e-ISSN : 2600-7924

Journal of Science and Technology

Numerical Performance of AlGaN/GaN High Electron Mobility Transistors under Hydrostatic Pressure and Temperature

Rajab Yahyazadeh [1*], Zahra Hashempour [1]

[1]Department of Physics, Khoy Branch, Islamic Azad University, P.O.Box: 175-58135, Iran

*Corresponding Author

DOI: https://doi.org/10.30880/jst.2020.12.01.003
Received 23 December 2019; Accepted 2 May 2020; Available online 14 June 2020

Abstract: In this paper, drain-source current, in AlGaN/GaN high electron mobility transistors have been investigated. In order to obtain parameters of exact AlGaN/GaN high electron mobility transistors such as electron density, the wave function, band gap, polarization charge, effective mass and dielectric constant, the hydrostatic pressure and temperature effects are taken into account. It has been found that the drain-source current decreases with increasing temperature and increases with increasing hydrostatic pressure. The increase in temperature is equivalent to a negative virtual gate and an increase in the hydrostatic pressure equivalent to the positive virtual gate voltage. Moreover, the temperature and hydrostatic pressure effective mass dependence in high electron mobility transistor structures are investigated, and it is observed that the increase of hydrostatic pressure decreases the effective mass and the wave function penetrated to quantum barrier AlGaN. The calculated results are in good agreement with existing experimental data.

Keywords: Temperature, Hydrostatic pressure, effective mass, AlGaN/GaN HEMTs,

1. Introduction

AlGaN/GaN heterostructure field-effect transistors (HFETs) have been interested in RF applications because of their outstanding high-frequency and high-power performance [1–3]. Linearity is one of the most crucial figures of merit for the application of power amplifiers. For improving the device linearity, advanced device structures or epitaxial structure engineering, such as field plate, nonlinear polarization dielectric, double-channel, and optimized barrier or cap layer thickness, has been explored [4–7]. The two-dimension electron gas (2DEG) in AlGaN/GaN interface is the major carrier for the high efficient electronic transport and was commonly assumed to be related to the piezoelectric polarization of the strained AlGaN layer and the spontaneous polarization. Understanding and controlling the transport behavior of carriers across the heterojunction interface is important for the optimization of their performance. Many reports have detailed the enhanced performance of piezotronic devices tuned by external mechanical strain/stress, including piezotronic enhanced photodetectors [8]. With the coupling of piezoelectric polarization with semiconductor properties in III-nitride materials, it suggests that III-nitride high electron mobility transistors (HEMTs) may be excellent candidates as strain- tunable transistors, and have potential applications in electromechanical sensing,

*Corresponding author: r.yahyazadeh@iaurmia.ac.ir

actuating, and mechanical energy harvesting. The current collapse through structural design and relieving the self-heating of the device are two effective efforts to tune/control the performance of AlGaN/GaN HEMTs [9]. More recently, the drain-source current of III nitride-based HEMT has been modeled by several groups [10-12]. It is important to investigate systematically the dependence of AlGaN–GaN HEMT performance on the hydrostatic pressure and temperature with including different physical parameters. In the present work, a new numerical model for the drain-source current of AlGaN/GaN HEMTs is presented. That is capable of determining effects of hydrostatic pressure and temperature on the effective mass, barrier thickness, band gap, drain-source current. One of the important advantages of this numerical method and the aspect of innovation in this work is the use of five important parameters effective mass, band gaps, lattice constants, dielectric constant, and barrier thickness that are simultaneously dependent on pressure and temperature. In addition, the effect of self-heating, multisubband, and polarization coulomb field scatterings on the mobility and electron density of quantum well used in the self-consistent solution of the Schrödinger equation. It should be noted that in this work atmospheric pressure is associated with hydrostatic pressure $\left(P = P_{hydro} + P_{atm}\right)$. That is, at zero hydrostatic pressure is the only atmospheric pressure applied and the fringing-field effect can be ignored.

2. Material and Method

In order to obtain accurate values for the Fermi energy, the energies of quantized levels within the 2DEG, potential profiles, wave function and the sheet carrier concentration for the 2DEG in AlGaN/GaN heterostructures; both the Schrödinger and Poisson equations must be solved self-consistently. This has been achieved by solving Schrödinger's equation and simultaneously taking into account the electrostatic potential obtained from Poisson's equation, as well as the image and exchange-correlation potentials using three-point finite difference method. The Schrodinger equation is introduced to solve the wave function of electrons in the quantum structures:

$$-\frac{\hbar^2}{2m_e^*}\nabla^2\psi_n + V\psi_n = E_n\psi_n \qquad (1)$$

where $\hbar$ represents the reduced Planck constant, m_e^* electron effective mass, V the potential function, ψ_n the nth state wave function, with its associated nth state energy level E_n. The electron effective mass m^* can be written as [14]

$$\frac{m_0}{m_e^*(P,T,m)} = 1 + \frac{E_P^\Gamma\left(E_g^\Gamma(P,T,m) + (2\Delta_{S0}/3)\right)}{E_g^\Gamma\left(E_g^\Gamma(P,T,m) + \Delta_{S0}\right)} \qquad (2)$$

where m_0 is the free electron mass, E_P^Γ is the energy linked to the momentum matrix element, Δ_{S0} is the spin-orbit splitting and $E_g^\Gamma(P,T,m)$ is the band gap variation as a function of the hydrostatic pressure and temperature. E_g^{AlGaN} , is given by [15-17]

$$E_g^{AlGaN}(T,P) = xE_g^{AlN}(T,P) + (1-x)E_g^{GaN}(T,P) - x(1-x) \qquad (3)$$

where E_g^{AlGaN} is the band gap from $E_g^{AlN}(T,P)$ and $E_g^{GaN}(T,P)$ respectively, as follows[16]

$$E_g(T,P) = E_g(0,0) + \gamma P + \sigma P^2 + \frac{\alpha T^2}{T + T_e} \qquad (4)$$

$E_g(0,0)$, stands for the band gap energy of GaN or AlGaN in the absence of the hydrostatic pressure and at a temperature 0K. The suggested parameters used in Eq. (4) in our calculations have been taken from Ref 14.

The Poisson equation relates the electrostatic potential with spatial charge distribution and it is written as

$$\kappa\nabla^2\varphi = -\rho + \nabla P_{tot} \qquad (5)$$

where φ is the potential distribution and ρ is the net charge which is a nonlinear function of the potential:

$$\rho(\varphi)=\left[p(\varphi)+n(\varphi)+N_D^+-N_A^-\right] \qquad (6)$$

p and n denote the mobile carrier density of holes and electrons, N_D^+ and N_A^- are the totally ionized donor and acceptor densities. $P_{tot}=P_{SP}+P_{PZ}$, denotes the total polarization vector that is composed of spontaneous polarization P_{SP} and strain-induced piezoelectric polarization P_{PZ}. By using the Al mol fraction (m), the lattice constant (a) and the strain (ϵ), they can be obtained as follows [18, 19]:

$$P_{GaN}^{PZ}=-0.918\grave{o}+9.541\grave{o}^2 \qquad (7)$$

$$P_{AlN}^{Pz}=\begin{cases}-1.808\grave{o}+5.624\grave{o}^2 & for\,\grave{o}<0\\ -1.808\grave{o}-7.888\grave{o}^2 & for\,\grave{o}>0\end{cases}$$

$$P_{AlGaN}^{SP}=0.090m-0.034(1-m)+0.21x(1-m)$$

The basal strain is expressed from the lattice of substrate a_s and the epilayer $a_e(T,P,m)$:

$$\grave{o}(T,P,m)=\frac{a_c-a_e(T,P,m)}{a_e(T,P,m)} \qquad (8)$$

The lattice constants as function of temperature, alloy and the hydrostatic pressure is given by [20, 21]

$$a_e(T,P,m)=a_0(m)\left[\left(1+\beta\left(T-T_{ref}\right)\right)\left(1-\frac{P}{3B_0}\right)\right] \qquad (9)$$

where $B_0=239GPa$ is the bulk modulus of sapphire. $\beta_{GaN}=5.56\times10^{-6}K^{-1}$ is the thermal expansion coefficient and $T_{ref}=300K^0$. $a_0(m)$, is the equilibrium lattice constant as a function of composition is given by [22, 23]

$$a_0(m)=0.13989m+0.03862 \qquad (10)$$

The piezoelectric polarization is defined by Vergard's law as

$$P_{AlGaN}^{Pz}=mP_{AlN}^{PZ}+(1-m)P_{GaN}^{PZ} \qquad (11)$$

The total polarization at the interface AlGaN/GaN is expressed as:

$$\sigma_s(T,P,m)=\left|P_{Al_mGa_{1-m}N}^{PZ}+P_{Al_mGa_{1-m}N}^{SP}-P_{GaN}^{SP}-P_{GaN}^{PZ}\right| \qquad (12)$$

2.1 Electron concentration

To calculate the total conduction electron concentration, the sheet density of electrons in each subband is found. The total density of electrons ($n=n_{2D}+n_{3D}$) that are the two and three-dimensional density electrons (n_{2D} and n_{3D}) is given as [24],

$$n_{2D}=\sum_i n_i=\sum_i\frac{m^*k_BT}{\pi\hbar^2}ln\left[1+exp\left\{\frac{\left(E_f-E_i\right)}{k_BT}\right\}\right]\left|\psi_i\right|^2 \qquad (13)$$

$$n_{3D} = \frac{2}{\sqrt{\pi} N_C F_{1/2}\left(\left(E_F - E_C\right)/k_B T\right)} \qquad (14)$$

Eq. (13) includes the density of each subband and gives the total sheet density of electron. Eq. (13) gives the three-dimensional electron density. Here, $F_{1/2}$ is Fermi integral of order 1/2.

Knowing the E_i, the $2DEG$ density and the Fermi energy can be calculated from these set of equations [25, 26]

$$n_{2D}\left(T,m,x,P\right) = \frac{\varepsilon_0 \varepsilon\left(m,T,P\right)}{\left(d_d\left(T,P\right) + d_i + \Delta d\right)}\left(V_{GS} - V_T - E_F - V_{CH}\left(x\right)\right) \qquad (15)$$

$$V_T = V_{BI} - \Delta E_c\left(m,T,P\right) - \frac{\sigma_{Pz}\left(m,T,P\right) d_d}{\varepsilon_0 \varepsilon\left(m,T,P\right)} - \frac{q N_D d_d^2}{\varepsilon_0 \varepsilon\left(m,T,P\right)} \qquad (16)$$

$$\varepsilon^{GaN}\left(T,P\right) = 10.28 \times exp\left(10^{-4}\left(T - T_0\right) - 6.7 \times 10^{-3} P\right) \qquad (17)$$

$$\varepsilon^{AlGaN}\left(m,T,P\right) = \varepsilon^{GaN}\left(T,P\right) + 0.03m \qquad (18)$$

$\varepsilon^{GaN}\left(T,P\right)$ and $\varepsilon^{AlGaN}\left(m,T,P\right)$ are the dielectric constant [27,28]. d_{AlGaN}, is the AlGaN barrier thickness [15,28]

$$d_{Al_mGa_{1-m}N}\left(T,P\right) = d_{AlGaN}\left(0\right)\left[1 - \left(S_{11}^{Al_mGa_{1-m}N} + 2S_{12}^{Al_mGa_{1-m}N}\right)P\right] \qquad (19)$$

where $d_{AlGaN}\left(0\right)$ is the AlGaN layer thickness without hydrostatic pressure and temperature variation. S_{11}, S_{12} are the elastic compliance constants of $Al_mGa_{1-m}N$ and they are given by [14, 28]

$$S_{11} = \frac{C_{11}C_{33} - C_{13}^2}{\left(C_{11} - C_{12}\right)\left[C_{33}\left(C_{11} + C_{12}\right) - 2C_{13}^2\right]} \qquad (20)$$

$$S_{12} = \frac{C_{12}C_{33} - C_{13}^2}{\left(C_{11} - C_{12}\right)\left[C_{33}\left(C_{11} + C_{12}\right) - 2C_{13}^2\right]}$$

$V_{CH}\left(x\right)$, is the channel potential and $\Delta d = 1/n_{2D}\int z n_{2D}\left(z\right)dz$ represents the effective width of the two dimensional quantum well [23]. ΔE_C, is the conduction band offset between AlGaN and GaN; It should be mentioned that to calculate the conduction band discontinuity in AlGaN/GaN interface, the temperature and hydrostatic pressure dependence of energy band gap has been taken into account as [16]:

$$\Delta E_C\left(T,P\right) = 0.75\left(E_g^{AlGaN}\left(T,P\right) - E_g^{GaN}\left(T,P\right)\right) \qquad (21)$$

2.2 Mobility

In order to obtain accurate values for mobility, the nonlinear formalism of the polarization–induced field as a function of Al mole fraction in AlmGa1-mN/GaN HEMTs have been assumed; moreover, intersub-band coupling coefficients $\left(H_{mn}\right)$ as well as all fully- and partially–occupied sub-bands within two dimensional quantum well are taken into account. From the definition of the drift mobility we obtain [29-31]:

$$\mu_{2DEG}(T,E)=\frac{e}{m^{*}}\tau_{total}(T,E)\ (22)$$

Where τ_{total} are the total relaxation times associated with PCF scattering and the other main scattering mechanisms. These relaxation times have been calculated using the methods described in Refs [29-32, 25]. Moreover, the different scattering rates can be separated into two types: (i) elastic scattering due to acoustic and piezoelectric phonons, ionized impurities and interface roughness, etc., and (ii) inelastic scattering due to polar optical phonons. In order to take into consideration all scattering mechanisms in the mobility calculation, it is necessary to include all such mechanism in the linearized Boltzmann equation and to solve it numerically using an iterative technique [33]. It should be noted that in the linearized Boltzmann equation, $\Phi(E,T)$ is the perturbation function so that to obtain the $\Phi(E,T)$ needs to take into account the contribution of all occupied sub-bands by means of following relation [34]:

$$\frac{1}{\Phi(E,T)}=\sum_{m}\sum_{n}\frac{n_m}{n_{2DEG}}\frac{1}{\Phi_{mn}}\qquad(23)$$

Equation (23) indicated that all occupied states contribute to the total mobility of the two-dimensional electron gases. This equation also shows that the contribution of each sub-band depends on its occupation number such that the most significant contribution comes from the first sub-band, which has the highest occupation number. Using such an approach, it is possible to calculate the 2D-electron mobility taking into account the combined contributions from each of the individual electron scattering mechanisms

2.3 Drain-Source Current

The drain-source current is given by the following relation [11, 12, and 23]:

$$I_{DS}=\begin{cases}Wqv(T,m,E)n_{2D}(V_{GS},x,m.T.P)-qD(T,E)\frac{dn_{2D}(V_{GS},x,m,T,P)}{dx} & Linear\ region\\ Wqv_{sat}(T,m)n_{2D}(V_{GS},x,m,T,P)-qD(T)\frac{dn_{2D}(V_{GS},x,m,T,P)}{dx} & saturation\ region\end{cases}\quad(24)$$

where the first term is the drift current and the second represents the diffusion current, W is the gate width, E is the electric field, $v(T,m,E)$ is the electron drift velocity and $D(T,m)$ is the electron diffusion constant which can be assumed to be related to the mobility via the classical Einstein relation for low field given by $D(T,m)=k_BT\mu(T)/q$ However, in order to solve Eq. (24), it is necessary to invoke the following, boundary condition at the source and drain ends of the channel region:

$$V_{ch}(0)=I_{DS}\times\left(R_S(V_{GS})+R_C\right)\qquad(25)$$

$$V_{ch}(L_{SG}+L_G+L_{GD})=V_{DS}-I_{DS}\times\left(R_D(V_{GS})+R_C\right)$$

Here contact resistance R_C is a constant value during the parameter measurement, the value variation of R_S results from the gate-source channel resistance. As a result, R_S and R_D are determined by the polarization coulomb field and other scattering mechanisms for the electrons in the gate-source channel [35, 36]. L_{SG}, L_G and L_{GD}, are the lengths of the ungated distance between source and gate, the gate length and the ungated distance between gate and drain, respectively. As it is inferred from the equations, the transport parameters of the 2-DEG are dependent upon temperature; however, the device temperature is different from the electron gas channel temperature because of SH effects. During the calculations, the SH effect has been taken into account as follows. The temperature difference between the channel and the bottom of the substrate ($\Delta T=T_{ch}-T_{sub}$) is [37]:

$$\frac{\Delta T}{T_{sub}} = \frac{\left(1-\left(P_{diss}/4P_0\right)^4\right)}{\left(1-P_{diss}/4P_0\right)^4} \quad (26)$$

where T_{ch} is the channel temperature and T_{sub} is the temperature of the substrate bottom.

where $P_{diss} = I_{DS}V_{DS}$ is the power dissipation, P_0 is referred to as a quality factor with power dimension

$$P_0 = \frac{\pi K_{GaN}\left(T_{sub}\right)WT_{sub}}{ln\left(8t_{sub}/\pi L_G\right)} \quad (27)$$

Here, t_{sub} is the thickness of the substrate, L_G is the gate length, and $K_{GaN}\left(T_{sub}\right) = 1.6\left(T_{Sub}/300\right)^{-1/4}$ is the thermal conductivity.

In the presented model, especially in calculating P_0, the following three assumptions are applied:

(a) The HEMT structure consists of two parts: the epitaxial layers and the substrate. In each part, the temperature changes smoothly.

(b) The AlGaN conduction region (parasitic channel) [11] is not considered as it is assumed since the applied V_{GS} is less than the critical voltage at which a parallel conduction path sets in the AlGaN layer. In other words, the thermal conductivity $\left(K_{AlGaN}\right)$ and electrical current $\left(I_{AlGaN}\right)$ of the AlGaN Layer was considered to be zero as P_0 depends only on the thermal conductivity of GaN.

(c) It is also assumed that the bottom temperature of the substrate linearly increases with the dissipated power, $T_{sub} = 300 + \lambda P_{diss}$. Here, λ is a parameter corresponding to the thermal resistance of the device package and can be calculated based on the device transconductunce [38, 39].

The above equations provide all the required parameters in order to calculate the drain current, extrinsic transconductance, and cut-off frequency. The calculation procedure is briefly described below:
(i) Given a set of drain-source currents, gate-source voltages, material parameters, and 2DEG effective width, the channel temperature and P_0 can be calculated.
(ii) Using this value of channel temperature, parameters such as 2DEG mobility, saturation velocity, and the other parameters in Eq. (9) can be calculated. For example, a new I_{DS} value can be determined.
(iii) When the new drain-source current has been determined, the carrier concentration of the quantum well channel can be re-calculated according to the channel voltage. Thus, new values for the effective width and the quantum well channel temperature can be obtained self-consistently.
(iv) The above procedure is repeated until I_{DS} converges to a solution, as presented in Figure 1 (the flowchart of the simulation algorithm).

2.4 Cutoff frequencies

Knowing the current-voltage characteristics, one can find small-signal parameters such as the extrinsic transconductance(g'_m), the drain conductance (g_d) and the gate-to-source capacitance(C_{GS}). The transconductance and drain conductance can be defined by differentiating I_{DS} with respect to V_{GS} and V_{DS}, where V_{DS} and V_{GS} are kept constant, respectively.
Knowing these parameters, one can calculate the cutoff frequency, f_T, which is calculated as[19]:

$$f_T(T,P,m)=\frac{g_m^{'}(T,P,m)}{2\pi\left(C_{GS}(T,P,m)+C_{GD}(T,P,m)\right)} \quad (28)$$

$$g_m^{'}(T,P,m)=\frac{g_m(T,P,m)}{1+g_m R_s(V_{GS})} \quad (29)$$

Three kinds of carrier concentration contribute to the gate-to-source (drain) capacitance. These are the carrier concentration for the two-dimensional electron gas, free carriers, and neutralized donors in the barrier layer. Therefore, the gate-to-source (drain) capacitance is given by [40, 41].

$$C_{GS}(C_{GD})=\sum_{k=0}^{3} qWL_G \frac{\partial n_k}{\partial V_{GS}(V_{DS})} \quad (30)$$

The subscripts 1, 2 and 3 refer to the 2DEG, free electrons and neutralized donors in the barrier layer, respectively.

3. Results and Discussion

In this paper, we present a numerical model for calculating the drain-source current of the AlGaN/GaN field effect transistors, which simultaneously investigates the influence of the hydrostatic pressure and temperature. To obtain a self-consistent solution of basic equations, iteration between the Schrödinger−Poisson equation systems is conducted by a three-point finite difference method. During the self-consistent calculation, A grid spacing as small as $1\times10^{-10}m$ along the z-axis and the convergent criteria for the electrostatic potential is set to be 0.1% to ensure the iteration convergence and stability of our calculation. Flow chart of the flow calculation program is solvable in a self-consistent manner according to Fig. 1. To assess the validity of the numerical model for the drain-source current a comparative study has been undertaken to compare theoretically obtained, I_{DS} and curves with experimental results. The experimental results, material and device details and all other material parameters have been taken from Refs13, 14, 16 and 17 for $Al_{0.24}Ga_{0.76}N/GaN$ HEMTs. Fig. 2 shows the dependence of AlGaN band-gap energy to the temperature and hydrostatic pressure. To investigate the physical concept of these effects, we first investigate the quantum well current density in terms of gate voltage at different pressures and temperatures. As shown in Fig. 2, the electron density of the quantum well and the threshold voltage decreases (the minimum voltage required for the quantum well). As temperature increases to 300K relative to the room temperature, the threshold voltage decreases by an absolute magnitude of 1V and an electron density of $1.65\times10^{16}m^{-2}$. The Figure of the insert in Fig. 2 indicates the electron density dependence on hydrostatic preassure at different gate voltages. As the hydrostatic pleasure increases to 30 Gpa relative to the atmospheric pressure, the threshold voltage increases by an absolute magnitude of 0.5 V and an electron density of $0.8\times10^{16}m^{-2}$. Since the threshold voltage depends on the total polarization charges (an important factor in the quantum well formation). Thus, as shown in Fig. 3, AlGaN polarization (Piezoelectric and spontaneous) and bound charge at the hetrointerface (σ_b) with the increase in hydrostatic pressure increase. With the increase in hydrostatic pressure, the lattice constants ($a_e(T,P,m), a_0(m)$) and occupancy of the various sub-bands (n_i) increase. This is due to the threshold voltage variations and the electron density of the quantum well. . According to the Fig. 4 at 300K and hydrostatic pressure 0GPa (atmospheric pressure), the band-gap energy of AlGaN is 3.8 eV. The band-gap energy decreases with increasing temperature and increases with increasing hydrostatic pressure. The main cause of these changes is related to the quantum well depth changes. As the pressure increases, the band discontinuity and the threshold voltage (Eqs.16 and 21) increases. But as the temperature increases, these two parameters decrease. By comparing the band-gap energy variations with respect to temperature and pressure, it is observed that hydrostatic pressure related changes are greater than temperature related changes. Fig. 5 shows the dependence of the energy gap of GaN to the temperature and hydrostatic pressure. The band-gap energy variations in this Figure are similar to the changes in Fig. 4. Fig. 6 shows the changes in the effective electron mass relative to the temperature and hydrostatic pressure. According to Fig. 6, with increasing temperature, the effective electron mass increases and decreases with increasing hydrostatic pressure. As the effective electron mass decreases, the mobility of

electrons in the quantum well increases. Therefore, an increase in the hydrostatic pressure is needed to increase the mobility of the electrons. Fig. 7 shows the electron wave functions in the quantum well in terms of distance in different gate voltages. z=0 is the AlGaN/GaN interface. In this figure, with the increase of the gate voltage, the electron wave functions and electron density of the quantum well increases. The Figure of the insert in Fig. 7 indicates the electron wave function impenetrable to the AlGaN barrier. In Fig. 8, the wave functions of the quantum well at different temperatures and constant hydrostatic pressure are shown. In this Figure, with increasing temperature, the height of wave functions and the corresponding electron density decrease. By comparing this Figure with Fig. 7, the temperature is as high as 600K; the electron density is decreased. As the figure shows, the increase in temperature causes more electron wave functions to penetrate the quantum barrier, leading to an increase in effective mass and a decrease in mobility and density. As the temperature rises to 600K, the penetration of wave functions rises from 3500 to 4800. In Fig. 9, the wave functions of the quantum well at different hydrostatic pressure and constant temperatures are shown. In this figure, with increasing hydrostatic pressure, the height of wave functions and the corresponding electron density increase. As the Figure shows, the increase in hydrostatic pressure causes decreases electron wave functions to penetrate the quantum barrier, leading to a decrease in effective mass and an increase in mobility and density. The increase in hydrostatic pressure of 30GPa; reduces the penetration of wave functions from 3800 to 2800. Fig. 10 shows the drain-source current variation in terms of the drain-source voltage AlGaN/GaN HEMTs at various temperatures and hydrostatic pressures. In the saturation region, there is a negative conductivity, which is a contribution to this decrease in the drain-source current due to the thermal effect and partly due to the influence of wave functions on the quantum barrier AlGaN that increases the effective mass at high drain-source voltage. According to this Figure, the temperature increase reduces the drain-source voltage. This decrease is higher in the saturation region than in the linear region, which is related to reduction electron wave functions, the electron density of quantum well, Increase effective mass and penetration of wave functions to the barrier. Increasing the hydrostatic pressure increases the piezoelectric polarization charge density and the drain-source current. Decreasing changes with increasing temperature relative to the incremental hydrostatic pressure changes are related to the effect of self-heating and the effect of penetration.

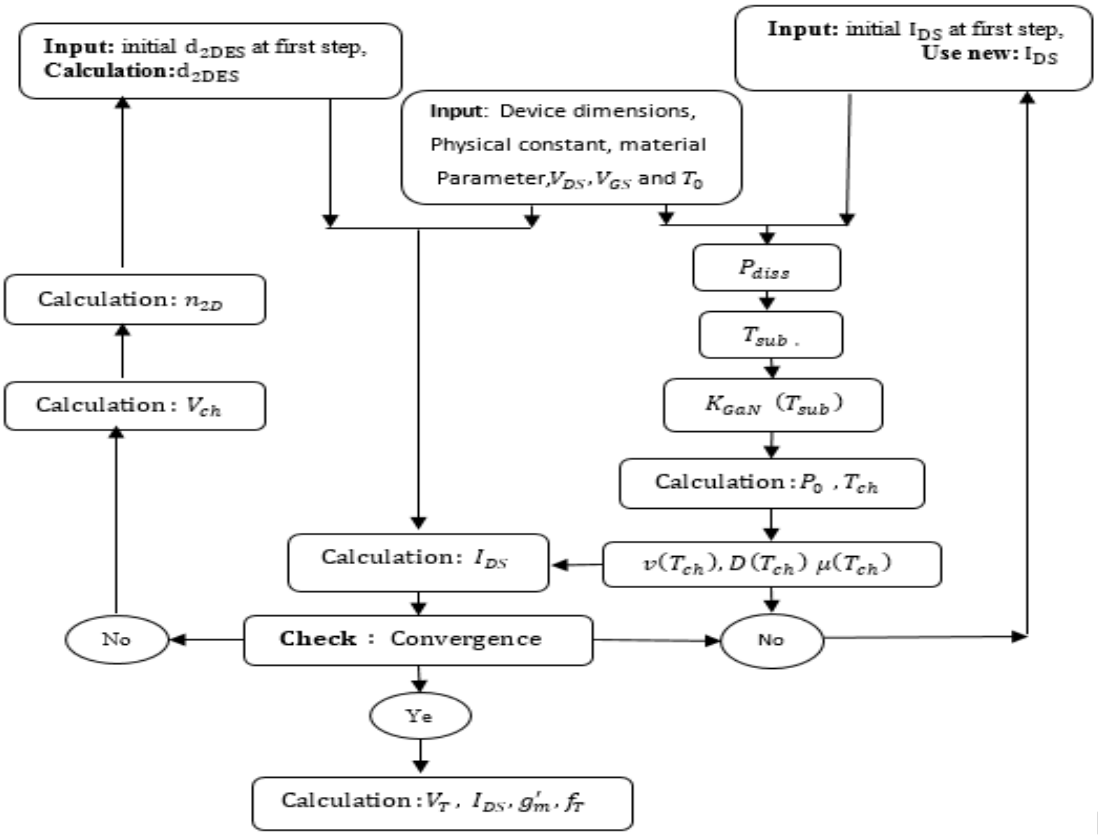

Fig.1 - The 2D transport model analysis steps

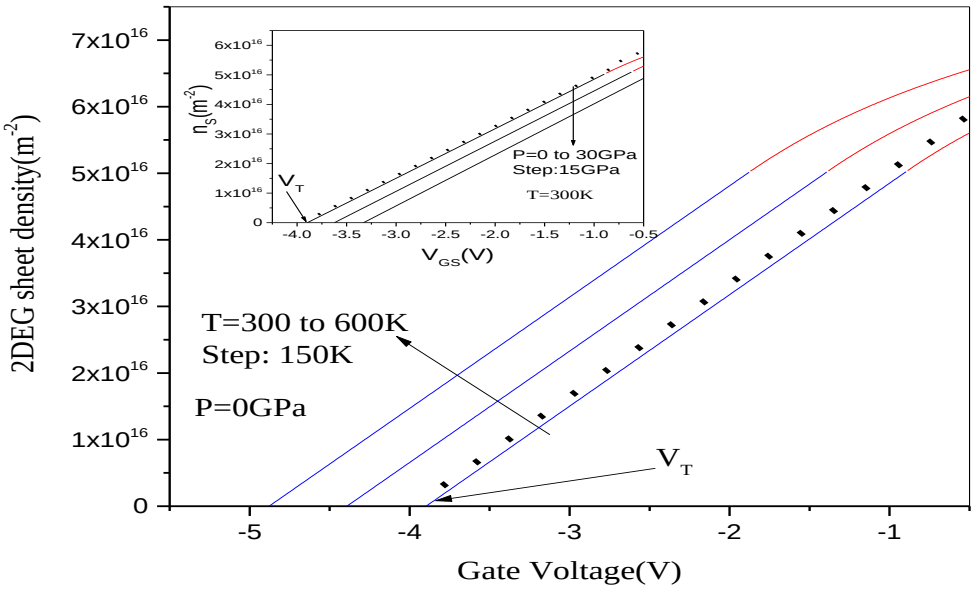

Fig. 2 - variations of the 2DEG sheet density as a function of Gate source voltage at different hydrostatic pressure. Insert: variations of the 2DEG sheet density as a function of Gate source voltage at different temperature. The experimental data (symbols) and other needed parameters have been taken from Ref [40]

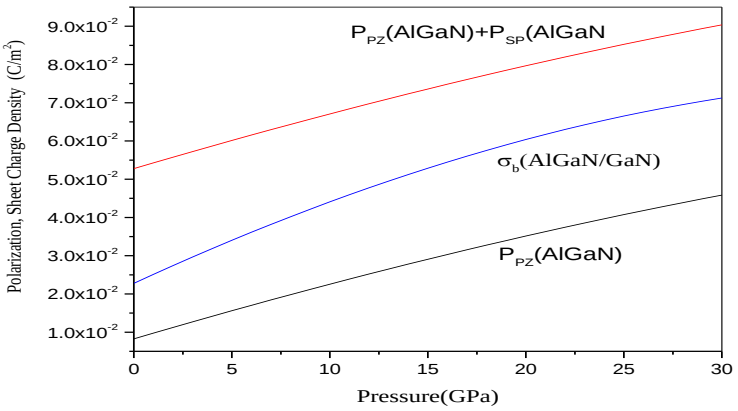

Fig.3 - The variation of AlGaN polarization (Piezoelectric and spontaneous) and bound charge at the hetrointerface(σ_b) as a function of the hydrostatic pressure.

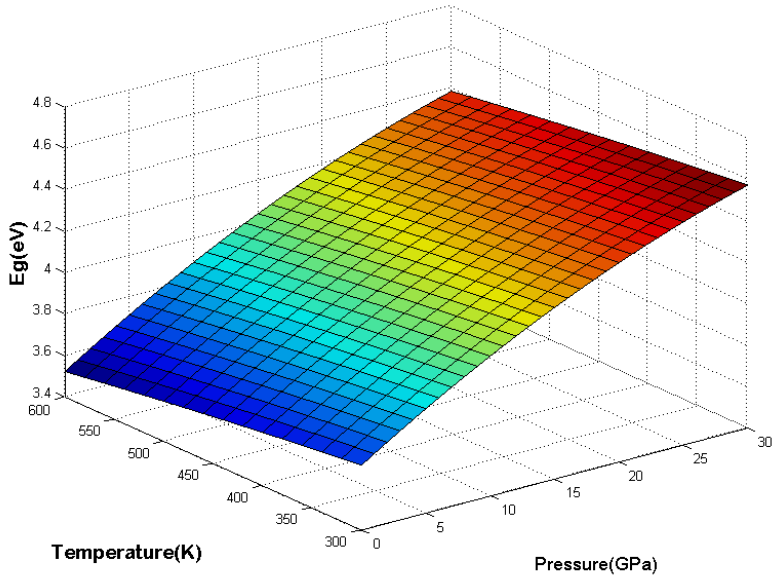

Fig. 4 - The band-gap energy of AlGaN as function of hydrostatic pressure and temperature for the $Al_{0.24}Ga_{0.76}N/GaN$ HEMTs

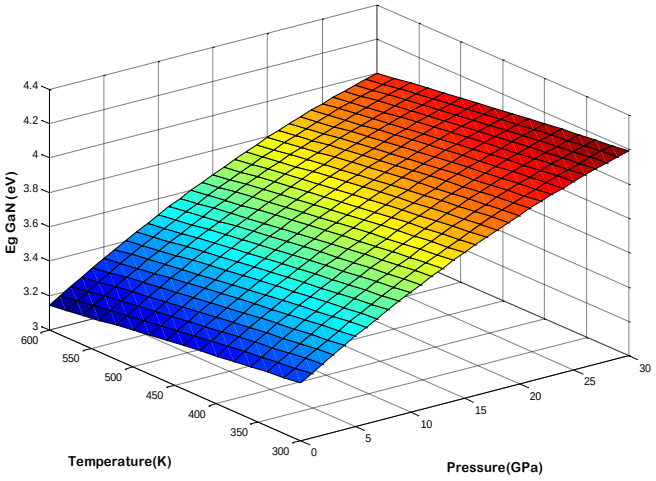

Fig.5 - The band-gap energy of GaN as function of hydrostatic pressure and temperature for the $Al_{0.24}Ga_{0.76}N/GaN$ HEMTs

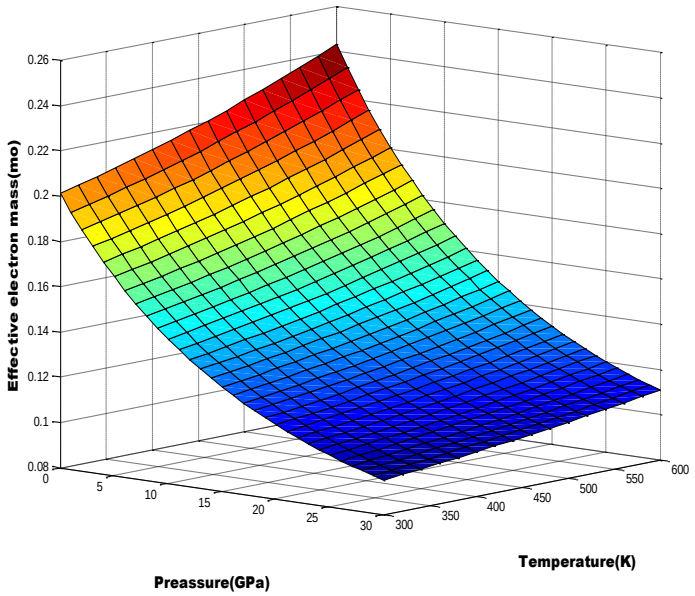

Fig. 6 - The effective electron mass of GaN as function of hydrostatic pressure and temperature for the $Al_{0.24}Ga_{0.76}N / GaN$ HEMTs

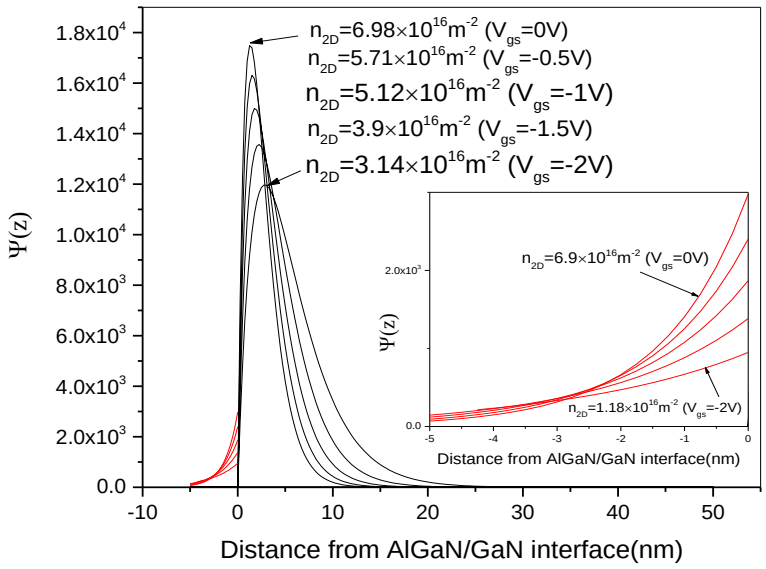

Fig. 7 - The electron wave function ψ(z) as a function of the distance from AlGaN/GaN interface under different n_{2D} (here n_{2D} corresponds to the electron density under the gate region as a function of gate bias)

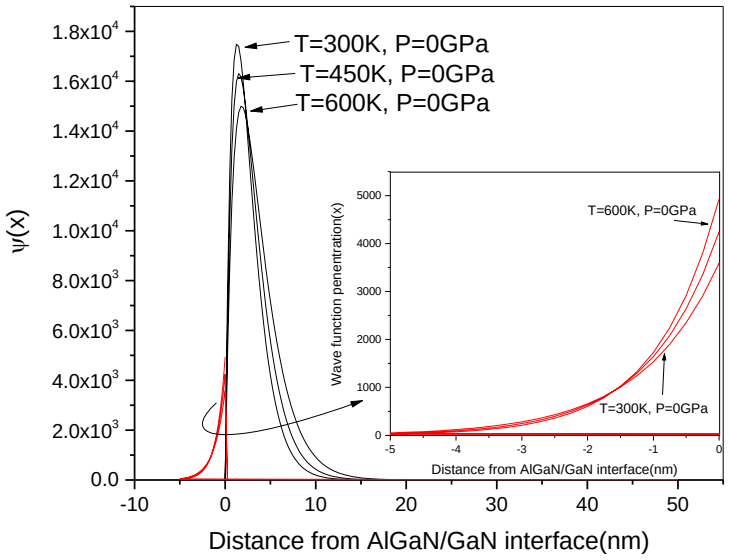

Fig. 8 - The electron wave function ψ(z) as a function of the distance from AlGaN/GaN interface under different temperature and without hydrostatic pressure. The insert indicates the electron wave function impenetrate to the AlGaN barrier

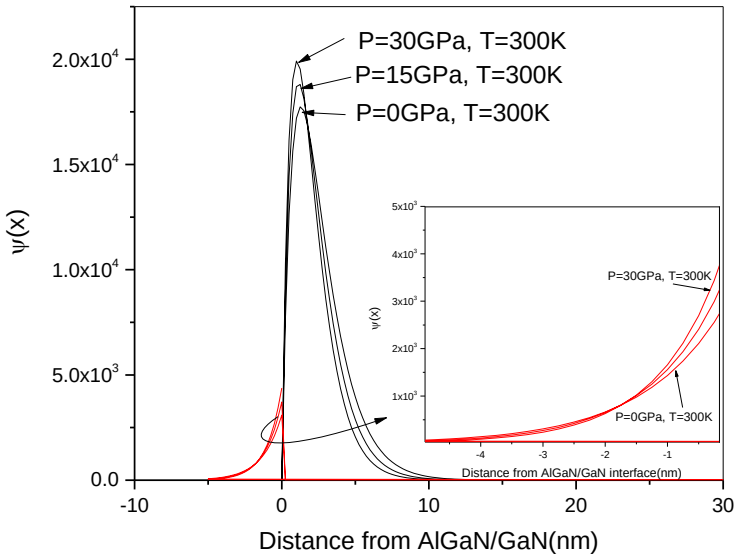

Fig. 9 - The electron wave function ψ(z) as a function of the distance from AlGaN/GaN interface under different hydrostatic pressure and without temperature. The insert indicates the electron wave function impenetrate to the AlGaN barrier

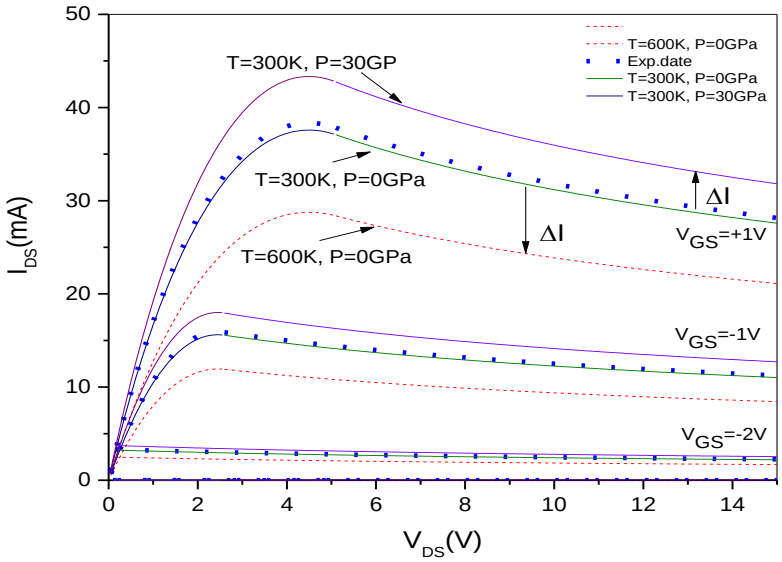

Fig. 10 - Drain current versus source–drain voltage for the $Al_{0.24}Ga_{0.76}N/GaN$ HEMTs, including temperature and temperature pressure effect in comparison with experimental data [13]

4. Conclusion

In this paper, an accurate numerical model has been developed for the drain-source current of AlGaN/GaN-based HEMTs. This model is able to accurately predict the dependence of drain-source current, electron density and effective electron mass on the temperature and hydrostatic pressure. From the results, it is apparent that the temperature is as high as 300; the electron density is decreased to $1.65\times10^{16}\,m^{-2}$ and the penetration of wave functions rises from 3500 to 480. This increase in temperature is similar to the virtual gate of -1V. The increase in pressure of 30GPa; reduces the penetration of wave functions from 3800 to 2800 and the electron density is increased to $0.8\times10^{16}\,m^{-2}$. This increase in hydrostatic pressure is similar to the virtual gate of +0.5V. Decreasing drain-source current with increasing temperature is related to the effect of self-heating and penetration to the quantum barrier but increasing drain-source current with increasing pressure is related to the piezoelectric polarization. This decrease is higher in the saturation region than in the linear region.

Acknowledgement

We are a faculty member of Islamic Azad University, Khoy Branch, and all resources are provided to our work through the University. The authors would like to thank Khoy Branch.

References

[1] Van der Geer, J., Hanraads, J. A. J., & Lupton, R. A. (2000). The art of writing a scientific article. Journal of Science Communication, 163, 51–59.
[2] Strunk, W., Jr., & White, E. B. (1979). The elements of style (3rd ed.). New York: MacMillan.
[3] Mettam, G. R., & Adams, L. B. (1999). How to prepare an electronic version of your article. In B. S. Jones & R. Z. Smith (Eds.), Introduction to the electronic age (pp. 281–304). New York: E-Publishing Inc.

[4] Fachinger, J., den Exter, M., Grambow, B., Holgerson, S., Landesmann, C., Titov, M., et al. (2004). Behavior of spent HTR fuel elements in aquatic phases of repository host rock formations, 2nd International Topical Meeting on High Temperature Reactor Technology. Beijing, China, paper #B08.
[5] Fachinger, J. (2006). Behavior of HTR fuel elements in aquatic phases of repository host rock formations. Nuclear Engineering & Design, 236, 54.